AL-TR-90-067

AD:

(2)

Final Report
for the period
16 Mar 1987 to
15 Sep 1990

Photochemical Preparation and Spectroscopic Characterization of H_4 and Its Decay Products

November 1990

Authors:
C.B. Moore
Y.T. Lee
A.H. Kung

University of California Berkeley
Chemistry Department
Berkeley CA 94720

F04611-87-K-0027

Approved for Public Release

Distribution is unlimited. The AL Technical Services Office has reviewed this report, and it is releasable to the National Technical Information Service, where it will be available to the general public, including foreign nationals.

Prepared for the: **Astronautics Laboratory (AFSC)**
Air Force Space Technology Center
Space Systems Division
Air Force Systems Command
Edwards AFB CA 93523-5000

NOTICE

When U. S. Government drawings, specifications, or other data are used for any purpose other than a definitely related Government procurement operation, the fact that the Government may have formulated, furnished, or in any way supplied the said drawings, specifications, or other data, is not to be regarded by implication or otherwise, or in any way licensing the holder or any other person or corporation, or conveying any rights or permission to manufacture, use or sell any patented invention that may be related thereto.

FOREWORD

This final report was submitted by the University of California Berkeley, Chemistry Department, Berkeley CA on completion of contract F04611-87-K-0027 with the Astronautics Laboratory (AFSC), Edwards AFB CA. AL Project Manager Dr Patrick Carrick.

This report has been reviewed and is approved for release and distribution in accordance with the distribution statement on the cover and on the DD Form 1473.

Patrick Carrick

PATRICK G. CARRICK
Project Manager

Stephen L. Rodgers

STEPHEN L. RODGERS
Chief, Applied Research in Energy Storage Office

FOR THE DIRECTOR

Robert C Corley

ROBERT C. CORLEY
Director, Astronautical Sciences Division

SECURITY CLASSIFICATION OF THIS PAGE

REPORT DOCUMENTATION PAGE

Form Approved OMB No. 0704-0188

1a. REPORT SECURITY CLASSIFICATION UNCLASSIFIED	1b. RESTRICTIVE MARKINGS
2a. SECURITY CLASSIFICATION AUTHORITY	3. DISTRIBUTION/AVAILABILITY OF REPORT Approved for Public Release; Distribution is unlimited
2b. DECLASSIFICATION/DOWNGRADING SCHEDULE	
4. PERFORMING ORGANIZATION REPORT NUMBER(S)	5. MONITORING ORGANIZATION REPORT NUMBER(S) AL-TR-90-067
6a. NAME OF PERFORMING ORGANIZATION University of California, Berkeley Chemistry Department 6b. OFFICE SYMBOL (*If applicable*)	7a. NAME OF MONITORING ORGANIZATION Astronautics Laboratory (AFSC)
6c. ADDRESS (*City, State, and ZIP Code*) Berkeley CA 94720	7b. ADDRESS (*City, State, and ZIP Code*) AL/LSX Edwards AFB CA 93523-5000
8a. NAME OF FUNDING/SPONSORING ORGANIZATION 8b. OFFICE SYMBOL (*If applicable*)	9. PROCUREMENT INSTRUMENT IDENTIFICATION NUMBER F04611-87-K-0027
8c. ADDRESS (*City, State, and ZIP Code*)	10. SOURCE OF FUNDING NUMBERS PROGRAM ELEMENT NO. / PROJECT NO. 5730 / TASK NO 003H / WORK UNIT ACCESSION NO. 344661

11. TITLE (*Include Security Classification*)
Photochemical Preparation and Spectroscopic Characterization of H_4 and its Decay Products (U)

12. PERSONAL AUTHOR(S)
Moore, C. Bradley; Lee, Yuan T.; and Kung, Andrew H.

13a. TYPE OF REPORT	13b. TIME COVERED	14. DATE OF REPORT (*Year, Month, Day*)	15. PAGE COUNT
Final	FROM 870316 TO 900915	9011	46

16. SUPPLEMENTARY NOTATION

17. COSATI CODES			18. SUBJECT TERMS (*Continue on reverse if necessary and identify by block number*)
FIELD	GROUP	SUB-GROUP	tetrahydrogen, electronic quenching, collision dynamics, photoionization, Rydberg states, hydrogen dimer
07	04		
20	10		

19. ABSTRACT (*Continue on reverse if necessary and identify by block number*)

Three areas of investigation on H_4 and its decay products are described:

(a) Studies of the effects of rotational and vibrational excitation on the rate of electronic quenching via the maximum ionicity excited state (MIES) for the system $H_2(B)$ + He, and on the rates for angular momentum reorientation for $H_2(B)$ in collision with He, Ne, Ar and molecular hydrogen are reported;

(b) A highly sensitive scheme for state-to-state detection of H_2 and an intense pulsed hydrogen cluster source were developed in an extensive but unsuccessful search for high-lying Rydberg states of the H_4 moiety;

(c) Results of a systematic investigation made to resolve rotational structures in the vibrational spectra of H_5^+ (H_2 molecules solvated in a H_3^+ core) show that additional work is required in order to obtain definitive identification of the rotational structures.

20. DISTRIBUTION/AVAILABILITY OF ABSTRACT	21. ABSTRACT SECURITY CLASSIFICATION
☒ UNCLASSIFIED/UNLIMITED ☐ SAME AS RPT. ☐ DTIC USERS	UNCLASSIFIED

22a. NAME OF RESPONSIBLE INDIVIDUAL	22b. TELEPHONE (*Include Area Code*)	22c. OFFICE SYMBOL
PATRICK CARRICK	805-275-5883	LSXP

DD Form 1473, JUN 86 *Previous editions are obsolete.* SECURITY CLASSIFICATION OF THIS PAGE

Table of Contents

List of Figures

List of Tables

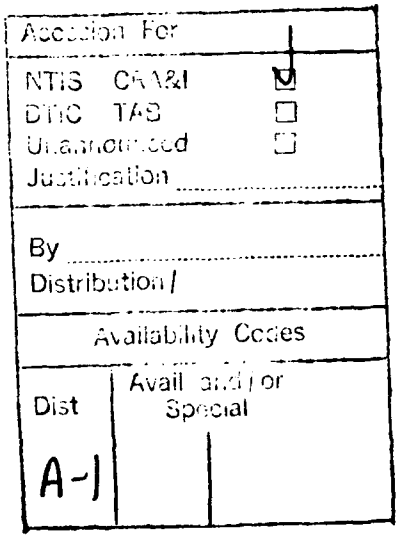

I. Introduction

Interest in the investigation of H_4 was initiated by the early quantum chemical calculations of Nicolaides and coworkers[1] that revealed the existence of a bound maximum ionicity excited state (MIES) of H_4. This opened up some significant possibilities, for if the MIES were stable, it could provide an energy density of 170 kcal/4 grams, corresponding to an Isp of 1700 sec. This Isp would make H_4 a prime candidate as a rocket propellent. In this report we describe experimental tests of the theoretical studies. These efforts include a detailed study of the molecular collision dynamics of B-state hydrogen and experiments on vuv and vuv + uv photoionization of hydrogen dimers. Recent theoretical work by the Nicolaides group and others shows that the MIES decays to $H_3(E)$ + H with a lifetime of 1-100 picoseconds,[2] which is extremely short for any practical purposes. The significance of the H_4 and H_2He systems therefore is now more of fundamental interest than of a prospective for rocket propulsion. Section II of this report gives an extended summary of the work on the effects of rotational and vibrational excitation on the rate of electronic quenching via the MIES for the system $H_2(B)$ + He, and on the rates for angular momentum reorientation for $H_2(B)$ in collision with He, Ne, Ar and molecular hydrogen. This series of studies provides important insights into the relaxation mechanism of B-state hydrogen and the formation and decay of the MIES. Section III describes experiments designed to search for Rydberg states of the H_4

moiety by vuv excitation of hydrogen dimers and trimers. The experiment produced a number of significant technological advances: the completion of an ultra-high resolution vuv laser source, the development of extremely sensitive REMPI state-to-state detection of ground state hydrogen, and the construction of an intense, pulsed hydrogen cluster source. In a related effort, a systematic investigation was made to resolve rotational structures in the vibrational spectra of H_2 molecules solvated in a H_3^+ core that is predicted by theoretical calculations. Details are described in section IV. Abstracts from available publications resulting from this work are attached in the appendices.

II. Molecular Collision Dynamics of B-State Hydrogen

The reactions of electronically excited $H_2(B\ ^1\Sigma^+_u)$ with $H_2(X\ ^1\Sigma^+_g)$ or He were chosen for study because of interest in the possibility of using stabilized H_2M^* (M = H_2(X) or He) as a high energy density material. Although later work indicated that the lifetime of H_2M^* was too short to be useful in this application, the system of H_2(B) + He still offers an ideal opportunity to understand the dynamics of MIES and to pursue a detailed study of the effects of rotational and vibrational quantum states on a reaction with a small activation energy. Using a linearly polarized laser to prepare H_2(B, v'=0, J'=1, M_J'=0) and monitoring the change in the spatial anisotropy of the fluore-

scence intensity with increasing pressure, it was possible to study the rates of elastic, reorienting collisions ($\Delta J=0, \Delta M_J=\pm 1$).

The relevant potential energy surfaces (pes) needed to describe the reaction of $H_2(B)$ with He are shown in Fig. 1. The reaction proceeds when $H_2(B)$ and He come together in the right geometry with enough energy to get over the barrier to reaction. The reactants enter the MIES minimum in the excited pes and may either undergo nonadiabatic transitions to the ground state pes or exit the well back to $H_2(B)$ + He. If a transition to the ground state pes occurs, both H atom and $H_2(X)$ products may be formed.

The first experiments performed examined the dependence of the reaction rate (the production of ground state products) on the vibrational and rotational state of the excited hydrogen reactant. The rates were determined by measuring the decrease in the laser induced fluorescence intensity with increasing pressure of He.

The results for $D_2(B, v'=0, J'=0-8)$ are shown in Fig. 2. There is clearly little dependence of the rate of reaction on the initial rotational state excited. These results are consistent with a picture of the reaction taking place preferentially when the angular momentum vector of the D_2 is aligned parallel with the relative velocity. The result is inefficient coupling of the rotational motion with the reaction coordinate, and the rotational energy may not be used to overcome the barrier to reaction.

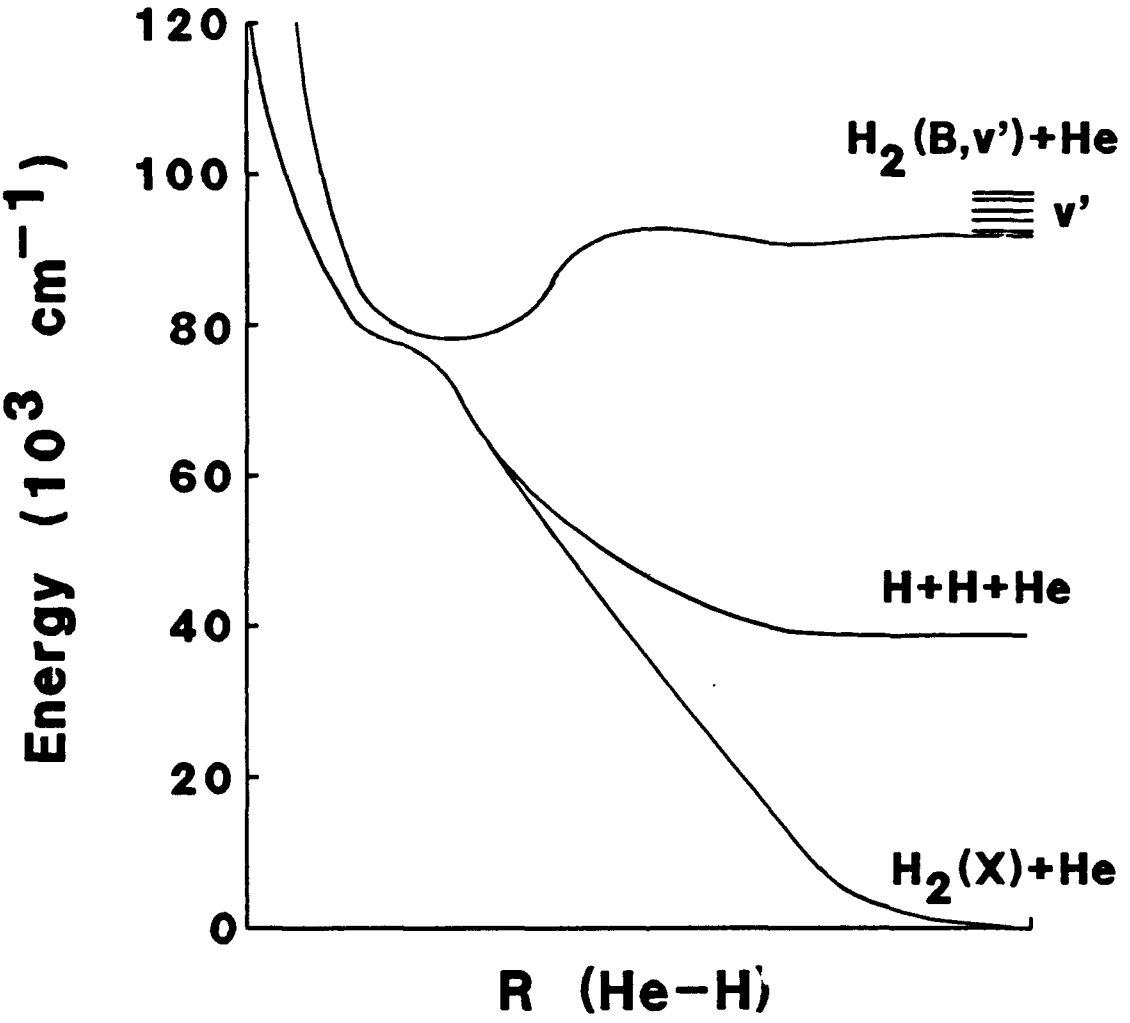

Figure 1. Schematic diagram of the potential energy surfaces involved in the quenching of B-state hydrogen. The excited hydrogen and helium cross a barrier on the excited potential energy surface; they then enter a deep well where the H-H bond length grows to about 2 Å. At the bottom of this well, there is a seam of avoided crossings with the ground state surface. Quenching is thought to occur when a non-adiabatic transition takes the metastable H_2(B)-He complex to the ground state surface, where the products are either H_2(X) and He or two H atoms and He.

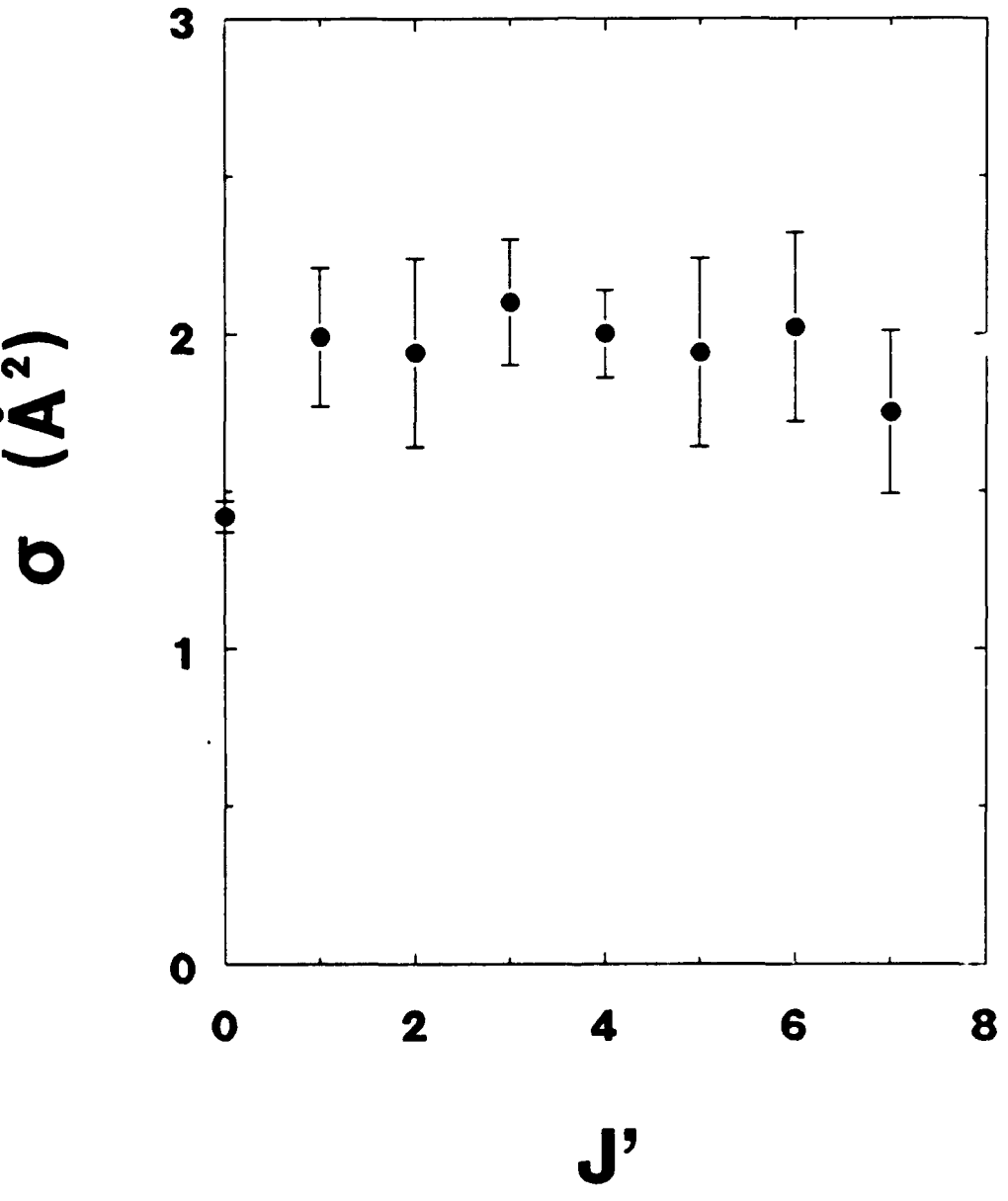

Figure 2. Rotational state dependence of the effective quenching cross sections for D_2 (v'=0). No significant change is seen for J' = 1 - 7.

The dependence of the reaction cross section upon vibrational excitation shows an increase in the cross section with increasing v′ up to v′=2, followed by a leveling off. The experimental results were fit using a vibrationally adiabatic model. Both the results and the fit are shown in Fig. 3. The initial increase in the reaction cross section with increasing vibrational excitation is due to a lowering of the barrier to reaction brought about by a decrease in the H-H stretching frequency at the transition state. The energy tied up in H-H stretching is less at the transition than for the free molecule. From the fit to the data, values for the barrier height of 250 ± 40 cm^{-1} and the decrease in the H-H stretching frequency of 140 ± 80 cm^{-1} were obtained. All of the experimental results are listed in Table I.

The second set of experiments performed, determined the rate constants for angular momentum reorientation of $H_2(B, v'=0, J'=1)$ in collisions with He, Ne, Ar and molecular hydrogen. The experiments were performed by measuring the decrease in the spatial anisotropy of the hydrogen B→X laser induced fluorescence intensity with increasing pressure of collision partner. The linearly polarized laser excites a population of $M_J'=0$ molecules. The molecules are aligned in space, and their fluorescence is spatially anisotropic. Collisions destroy the initial alignment, $M_J' = \pm 1$ are populated, and the fluorescence becomes more isotropic. By increasing the pressure of the collision partner and monitoring the decrease in the fluorescence anisotropy, the

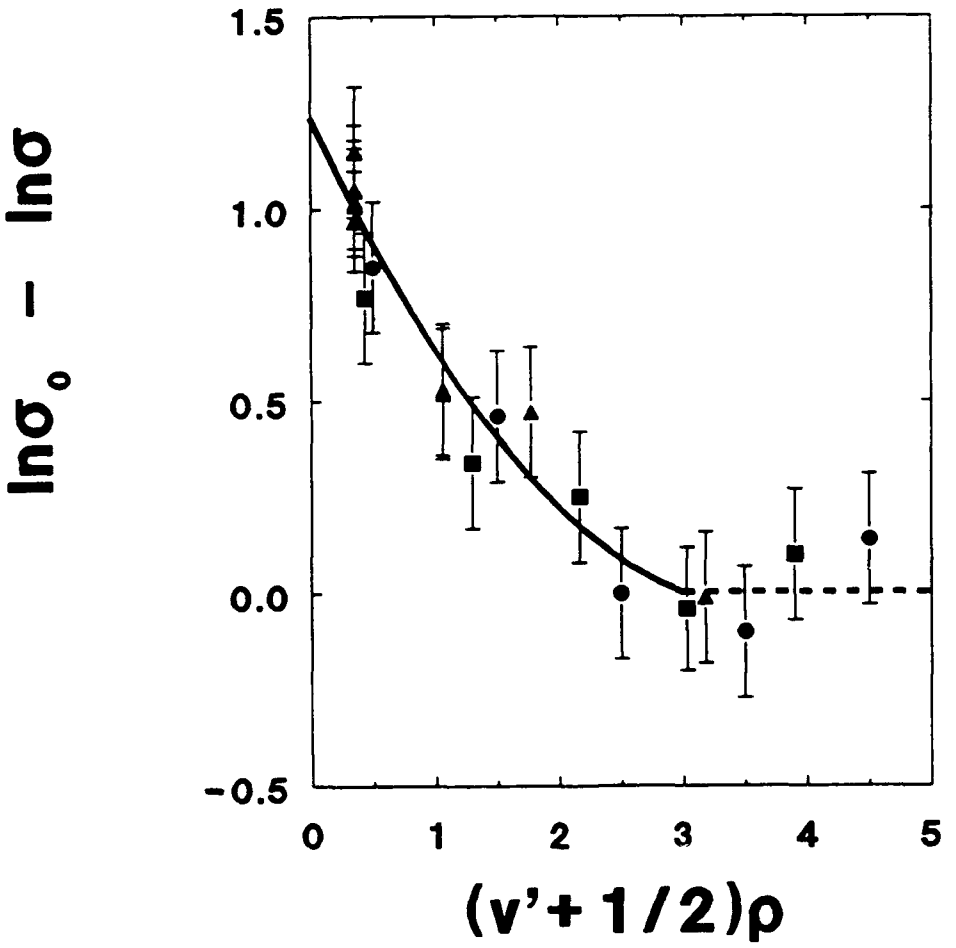

Figure 3. Experimental data and the fit to the data assuming a vibrationally adiabatic description of the barrier to complex formation for He + $H_2(B)$. The symbols are: triangles for D_2, squares for HD, and circles for H_2. The ($v'=0,J'=0$) data have been excluded, and the points for D_2 ($v'=0$) and D_2 ($v'=1$) represent averages of the data for non-zero J'. The solid line is the best fit to the data, and the dashed line is drawn where $V_b = 0$. The parameters from the best fit to the data give a barrier height of 250 cm^{-1} (the barrier on the electronic pes plus the zero-point energy in the bending vibration at the barrier) and a difference in the vibrational frequencies between $H_2(B)$ and the H-H stretch at the transition state of 140 cm^{-1}.

rates for the reorienting collisions may be determined. Typical experimental results are shown in Fig. 4, and the results are summarized in Table II. All of the cross sections for reorientation are quite large; this is a result of the large anisotropy of the $H_2(B)$-M pes (Fig. 5). Semiclassical calculations were carried out to model the reorientation of the angular momentum, and a value for the reorientation cross section of 20 $Å^2$ was obtained. The discrepancy between the experimental and calculated values is most likely due to inadequacies in the semiclassical treatment.

III. Search for Metastable H_4 via vuv excitation of $(H_2)_n$

It has been shown in experiments completed in our laboratory that when vacuum uv photons excite H_2 molecules in $(H_2)_2$ to a Rydberg state, intramolecular processes efficiently produce H_3^+ + H + e.[3] This formation of H_3^+ can be observed below the ionization threshold for H_2 where the process must be

$$(H_2)_2 + \text{vuv} \dashrightarrow H_2^{\bullet}H_2 \dashrightarrow (H_2 H_2)^+ + e \dashrightarrow H_3^+ + H + e.$$

Since the calculated structure of the H_4 molecule in its metastable state is $H_3^+ H^-$ and is $(H_3^+ H)^-$ in its Rydberg states, vuv excitation of the van der Waals molecule to a high lying Rydberg state $(H_2)_2^{**}$ followed by intramolecular chemical relaxation and photoemission offer a highly possible route to observe the existence of metastable H_4 molecules. The excitation to high

Table 1. Observed quenching rate constants and effective quenching cross sections.

$\|v',J'\rangle$	Pumping Transition	k_Q[a] (cm^3/molecule-s) $\times 10^{11}$	$\langle\sigma\rangle$ ($Å^2$)
		D_2	
$\|0,0\rangle$	P(1)	2.51 ± 0.09	1.42
$\|0,1\rangle$	P(2)	3.52 ± 0.39	1.99
$\|0,2\rangle$	P(3)	3.43	1.94
$\|0,3\rangle$	R(2),P(4)	3.70 ± 0.35	2.10
$\|0,4\rangle$	R(3),P(5)	3.53 ± 0.25	2.00
$\|0,5\rangle$	R(4)	3.43	1.94
$\|0,6\rangle$	R(5)	3.56	2.02
$\|0,7\rangle$	R(6)	3.09	1.75
$\|1,3\rangle$	P(4)	5.72	3.24
$\|1,4\rangle$	P(5)	5.83	3.30
$\|2,6\rangle$	P(7)	6.10	3.46
$\|4,3\rangle$	P(4)	9.79	5.56
		HD	
$\|0,0\rangle$	P(1)	3.94	2.07
$\|0,3\rangle$	R(2)	4.85	2.55
$\|1,2\rangle$	P(3)	7.50	3.94
$\|2,5\rangle$	P(6)	8.21	4.31
$\|3,0\rangle$	P(1)	11.2	5.90
$\|4,3\rangle$	P(4)	9.47	4.98
$\|3,2\rangle$	R(1)		9.90[b]

Table I. (continued)

$\|v',J'\rangle$	Pumping Transition	k_Q[a] (cm^3/molecule-s) $\times 10^{11}$	$\langle\sigma\rangle$ ($Å^2$)
		H_2	
$\|0,0\rangle$	P(1)	4.10	1.90
$\|0,3\rangle$	R(2)	5.09	2.36
$\|1,1\rangle$	P(2)	7.08	3.50
$\|2,5\rangle$	P(6)	12.0	5.54
$\|3,1\rangle$	P(2)	14.0	6.51
$\|4,3\rangle$	P(4)	10.4	4.82

[a] Uncertainties ($\pm 2\sigma$) are 15%, unless given.

[b] E. H. Fink, D. L. Akins, and C. B. Moore, J. Chem. Phys. **56,** 900 (1972).

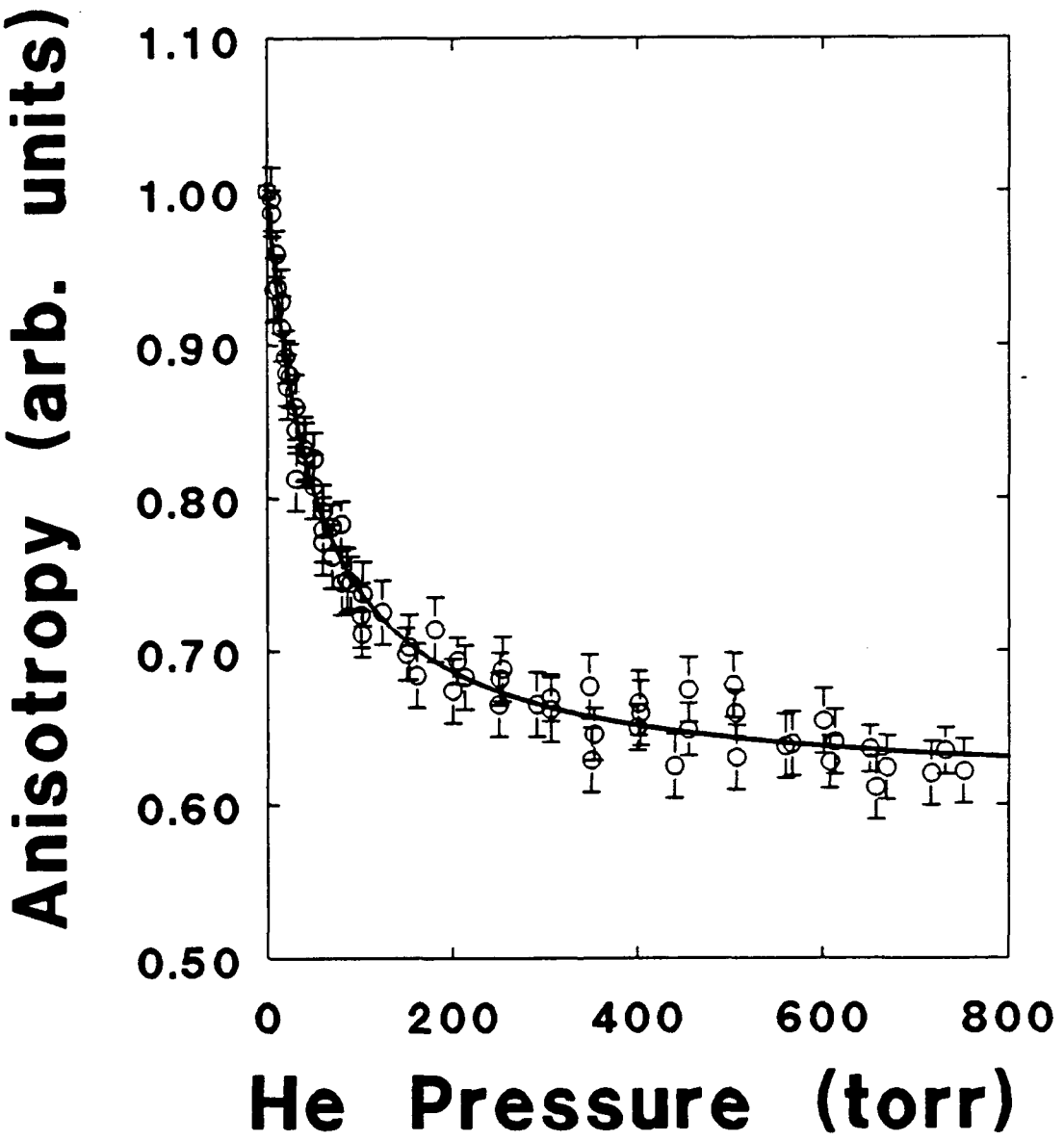

Figure 4. Reorientation data for HD with He as collision partner is shown here. The solid line is the best- fit to the data. The error bars represent the larger of either the standard deviation of the mean of the three measurements at a given pressure or the standard deviation of the mean expected using the standard deviation of the more numerous low pressure measurements.

Table 2. Angular momentum reorientation rate constants and effective cross sections.

System	k (cm^3 $molecule^{-1}$ s^{-1}) $\times 10^{10}$	σ ($Å^2$)[a]
H_2 - He	6.41	29.7 ± 7.4
HD - He	5.10	33.2 ± 5.0
D_2 - He	4.85	27.6 ± 10.8
H_2 - Ne	4.95	26.8 ± 7.0
HD - Ne	5.16	33.5 ± 7.4
D_2 - Ne	4.23	31.0 ± 9.2
HD - Ar	1.57	10.6 ± 2.0
D_2 - Ar	1.83	13.9 ± 3.0
$D_2(B)-H_2$	1.65	7.6 ± 3.4

[a] All uncertainties are ± 2 standard deviations from the fit to the data.

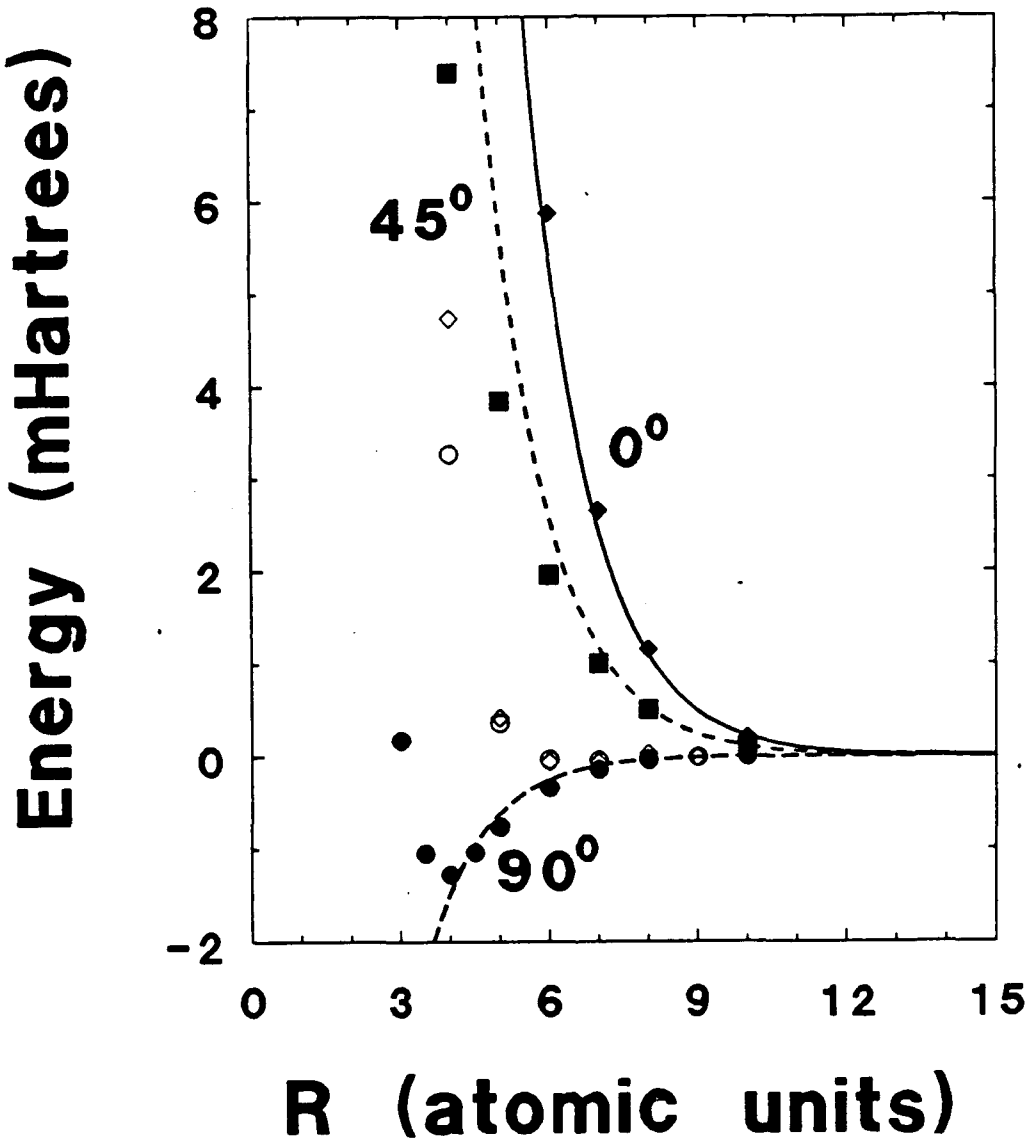

Figure 5. The ab initio data of Römelt, et al. for the H_2(B)-He potential energy are shown for: collinear approach (black diamonds), 45Å approach (black squares) and perpendicular approach (black circles). Also shown are the ab initio data for the H_2(X)-He potential for: collinear (open circles) and perpendicular (open diamonds) approach. The much higher anisotropy of the H_2(B)-He potential is readily apparent.

broadening of Rydberg state transitions of the H_2 molecule that is embedded in a dimer or trimer molecule. The formation of H_3^+ from the exictation can be detected easily lying Rydberg states of $(H_2)_2$ can be evidenced by frequency shifts and/orand if metastable H_4 molecule is formed by emitting a visible photon, H_4 can be detected by photoionization which eventually will form H_3^+. The experimental studies can best be carried out by photoionization in a pulsed molecular beam setting.

The experiment requires development of a highly sensitive technique to detect H_2 and $(H_2)_n$ molecules. The technique involves use of a broadly tunable vuv source which was developed in our laboratory.[4] Figure 6 shows a schematic of one of two identical arms of the laser setup. In the course of this study we demonstrated that (1 + 1) resonance-enhanced multiple photon ionization (REMPI) is an extremely sensitive scheme for the detection of H_2.[5] A detection sensitivity of 10^5 molecules/state/cm^3 was demonstrated. This number sets the lower limit of detectivity for the existence of the H_4 molecule in our experiment.

The ionization threshold for H_2 dimers is at ~88 nm, red-shifted from the threshold for H_2 which is at 80.4 nm. Ionization resonances that appear at wavelengths longer than 80.4 nm could then be associated with the dimer. Furthermore, excitation at wavelengths longer than 88 nm followed by laser induced ionization would allow identification of Rydberg series of the dimer. The relevant region of investigation for this experiment is therefore approximately from 80nm to 90nm. Radiation in this region was

generated by resonant 2 + 1 four-wave mixing in xenon. Using 2 mj at 222 nm and 4-5 mj at ~450 nm. approximately 10^9 photons with a bandwidth of 0.5 cm^{-1} was delivered to the interaction region.

A liquid-nitrogen cooled pulsed molecular beam source was developed for this experiment. Figure 7 shows a cross-section of the nozzle design. The critical aspect is the use of a long stainless steel tubing with a small diameter which serves to thermally isolate the cooled region at the tip of the nozzle from the body which needs to be close to room temperature for the piezoelectric crystal to function adequately. The other feature of this beam source is its high throughput which provides a high flux of Van der Waals molecules for investigation. Figure 8 shows a vuv laser-mass spectrometry trace of a pulsed beam of $(H_2)_n$ produced by this nozzle source. Only odd mass ions were observed. These were the stable ions. No even mass ions were observed although some effort was spent to look for H_4^+. In subsequent experiments the H_2 backing pressure was adjusted so that the beam consists of approximately 90% monomers and 10% dimers.

Spectral scans were made with the nozzle at liquid nitrogen temperature and at room temperature over the regions around 80 nm, 84 nm, and 88.9-90.5 nm. in search for ionization resonances that would give evidence to the presence of highly excited H_4 Rydberg states. The H_3^+ product was monitored. Figures 9, 10, and 11 are representative traces of the results of these scans. There were several resonance peaks, especially in the region 88.9 nm to 90.5 nm. Careful analysis of the peak positions and widths show that the majority of these peaks correspond to molecular hydrogen

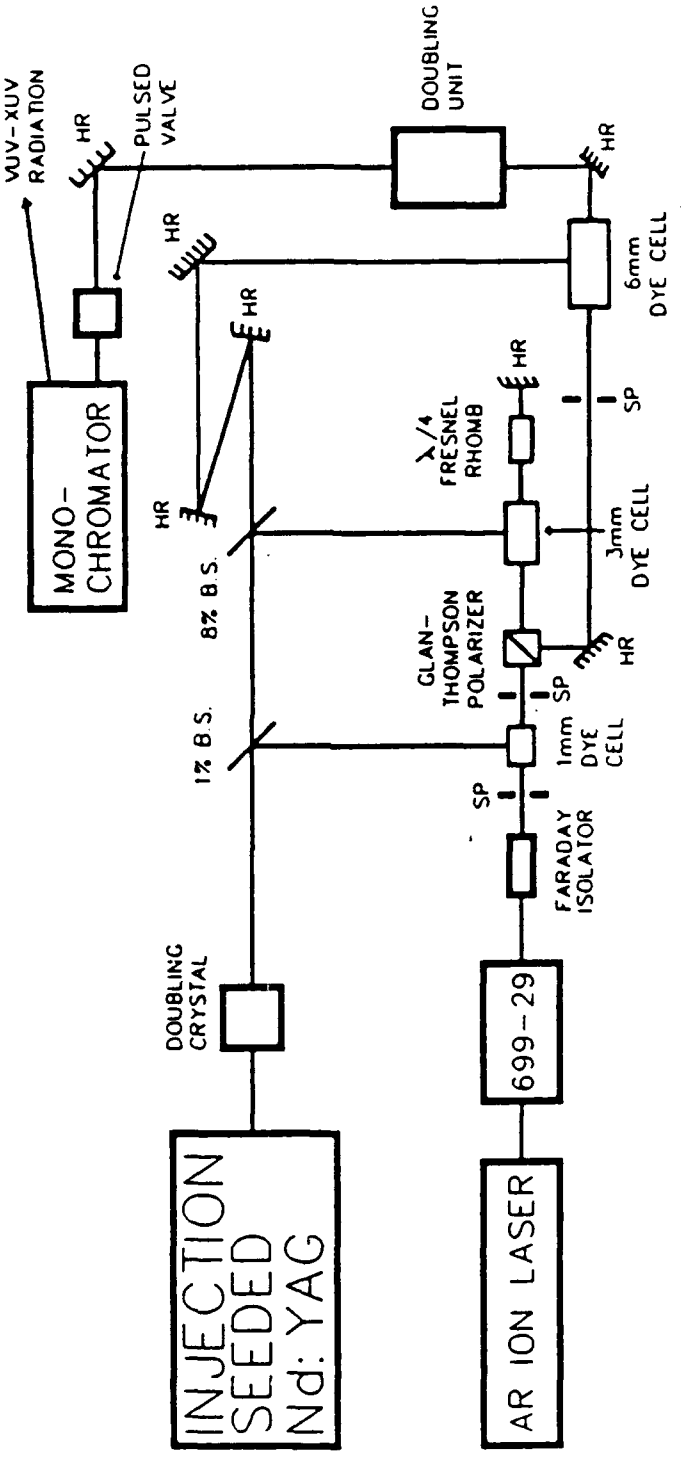

Figure 6. Schematic of the one arm of the vuv laser source. The vacuum chamber for the experiment is attached to the exit of the monchromator. (BS=beam splitter, HR=high reflecting mirror, SP=spatial filter/telescope)

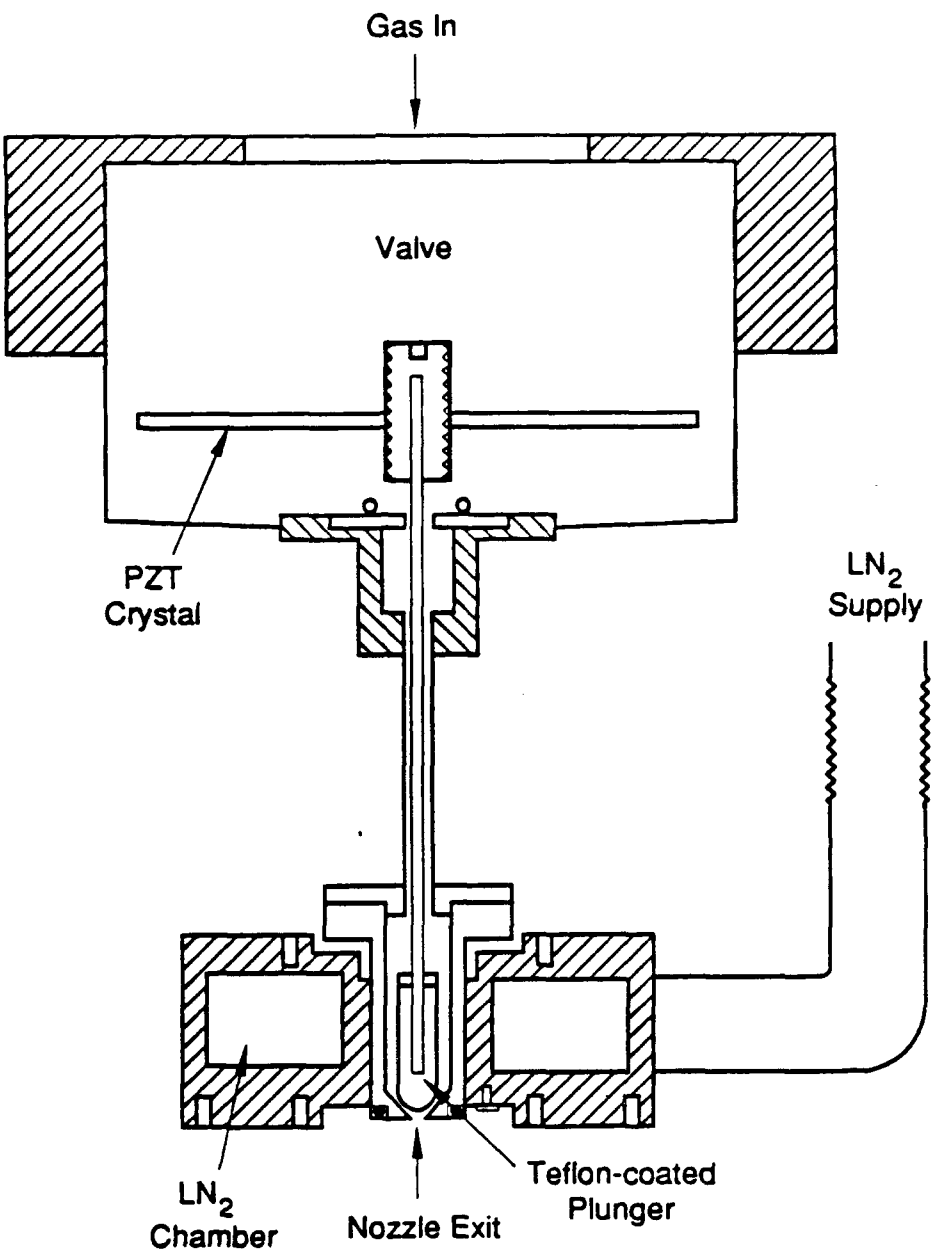

Figure 7. Cross-sectional view of the modified pulsed nozzle. A thin stainless tubing extends the nozzle exit from near the valve body to a distance 2" away. The plunger is made of copper overcoated with teflon to maintain sealing of the nozzle at liquid nitrogen temperature.

transitions that were recorded simultaneously. The remaining peaks also appeared in room temperature scans and can be attributed to HD transitions. Table III is a summary of the observations.

The source of the H_3^+ signal can be explained as produced by ion-molecule reactions of resonantly ionized H_2 with molecular hydrogen in the beam. We estimated that ion-molecule reactions would produce about 0.5 ion counts per laser shot, which is in agreement with the observations. The HD^+ peaks must originate from the 0.015% natural abundance of HD in the sample. These observations set an upper limit in the production of metastable Rydberg states of the H_4 molecule. The most likely possibility for the absence of sharp features identifiable to H_2 dimer excitation is predissociation of the excited dimer to $H + H_3$, which in turn dissociates to $H + H_2$. The results indicate that the predissociation lifetime is at least 1000 times faster than the lifetime of the corresponding H_2 state, which puts the lifetime in the picosecond regime. In other words, the original premises of producing metastable H_4 from highly excited Rydberg states will not be effective.

More experiments are required to substantiate this possibility. One approach to show that this is indeed the case is to probe the H atoms formed. This will require a second vuv laser tuned to a H atom resonance which introduces significant experimental complexity. Meanwhile, our results are in agreement with the detailed theoretical calculations performed by other groups who showed that the H_4 molecule is highly unstable.

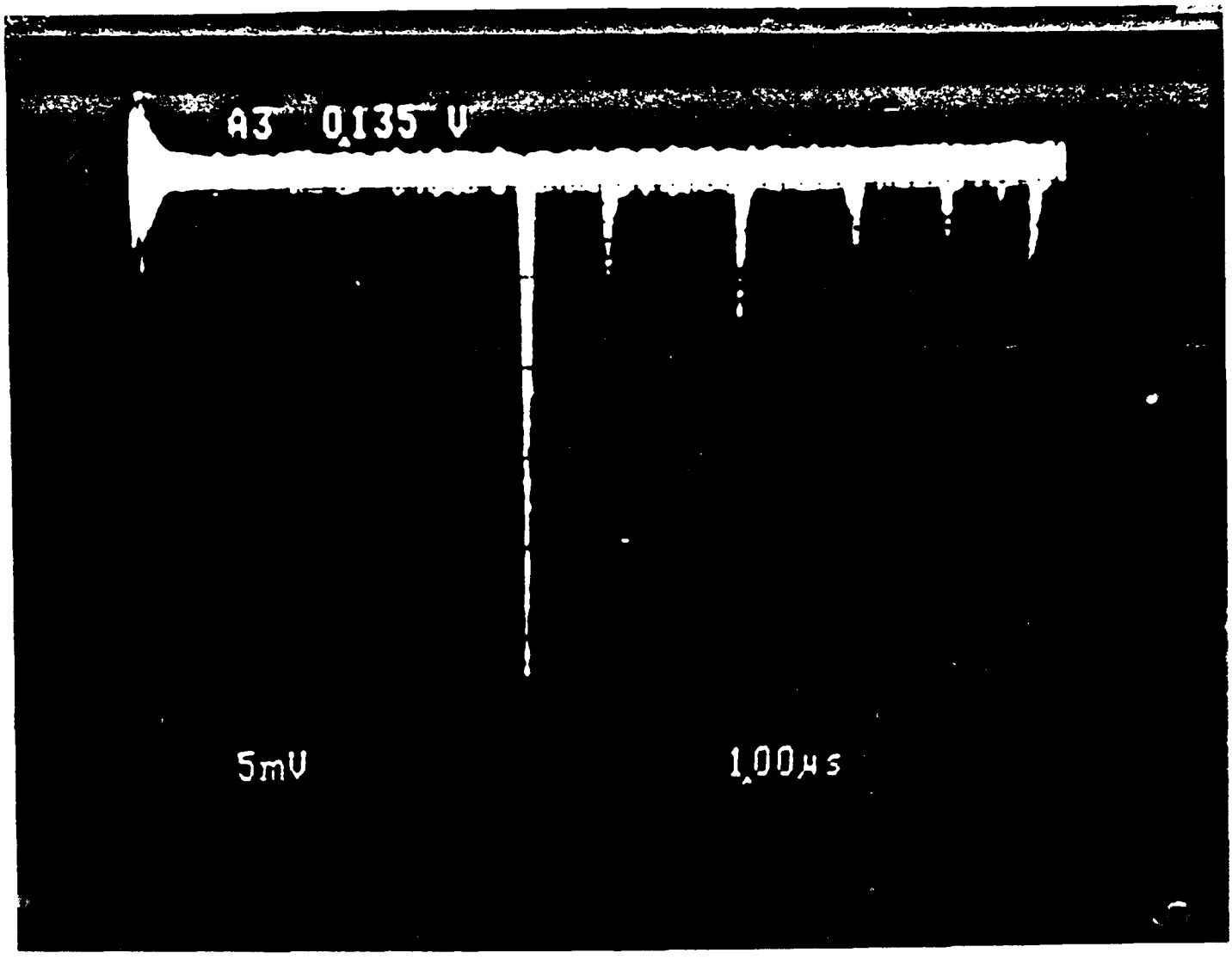

XBL 909-3208

Figure 8. Oscilloscope trace of the TOF mass spectrum of the H_2 cluster source, showing ion signal assignable to masses of, from left, 2,3,5,7,9 and 11. The cluster ions are produced by direct vuv ionization at 74 nm of $(H_2)_n$.

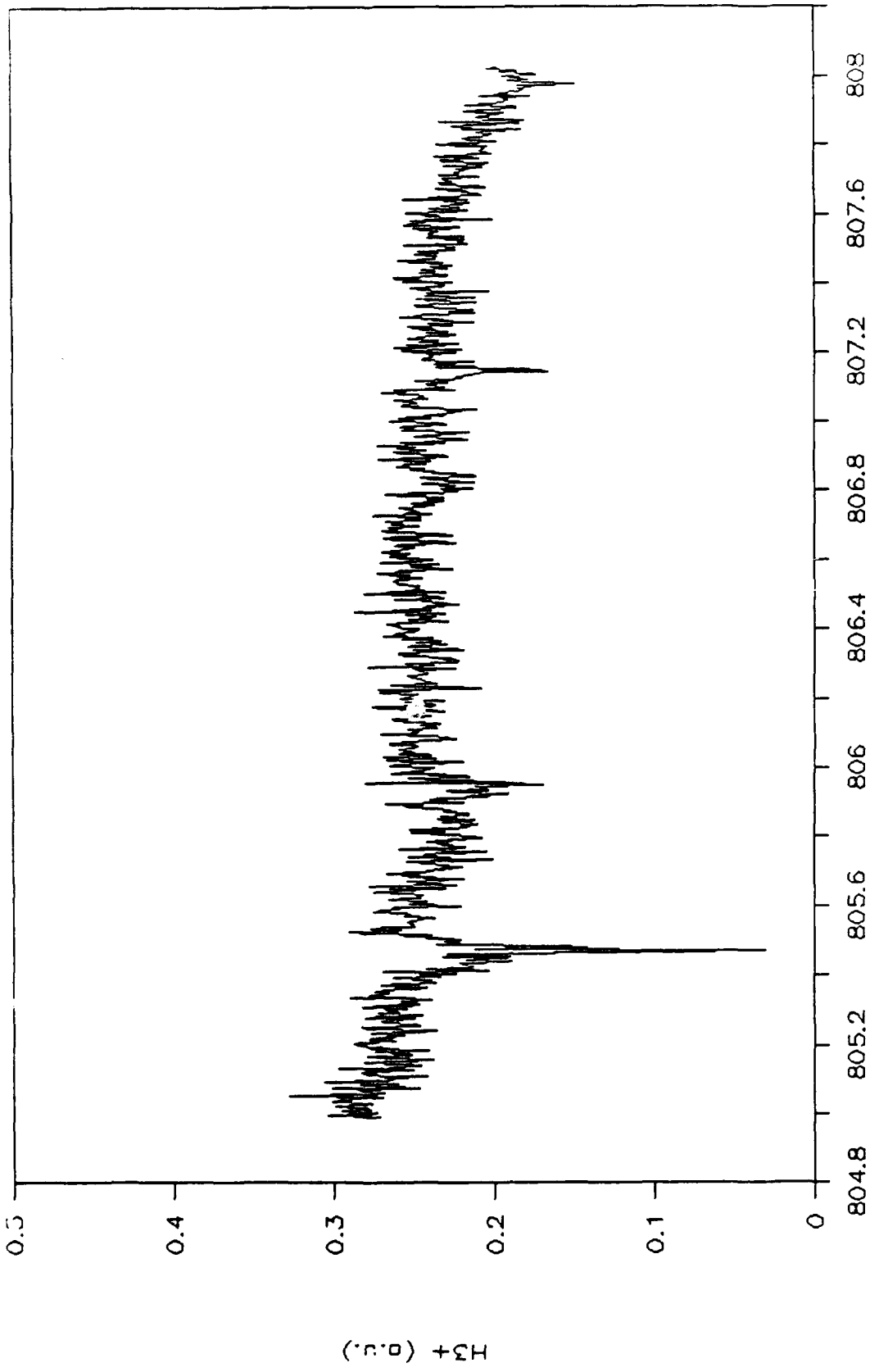

Figure 9. Photoionization spectrum of $(H_2)_2$ from 80.5 nm to 80.8 nm. The high frequency noise is due to statistical noise. Major dips correspond to drops in vuv power at those wavelengths. Baseline is at 0.02 in the vertical scale, which is in arbitrary units.

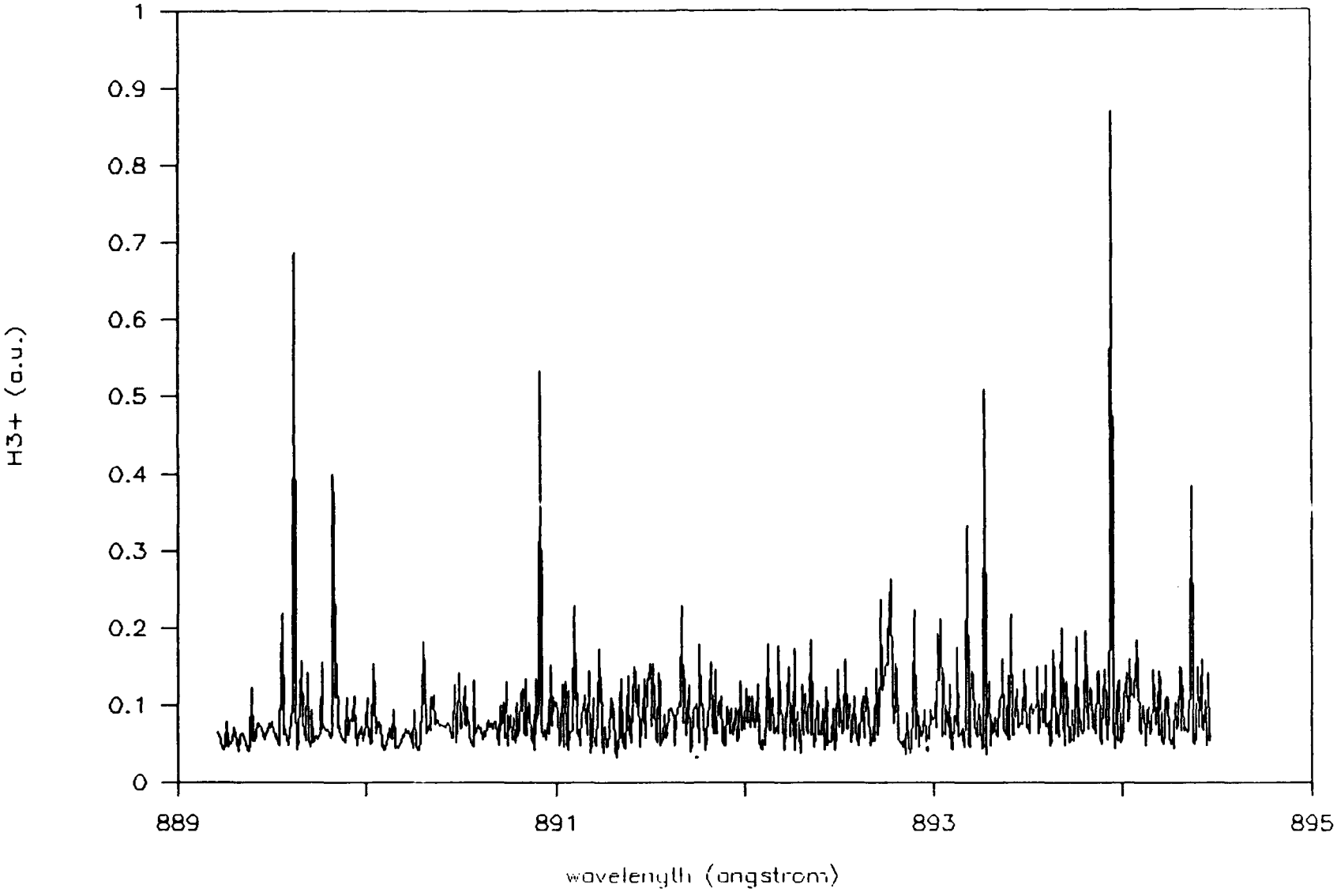

Figure 10. Photoionization spectrum of $(H_2)_2$ from 88.9 nm to 89.45 nm obtained by ion counting detection. Maximum signal in this spectrum corresponds to approximately 0.5 count per laser shot. Calibration shows that 0.1 count per laser shot constitutes real signal.

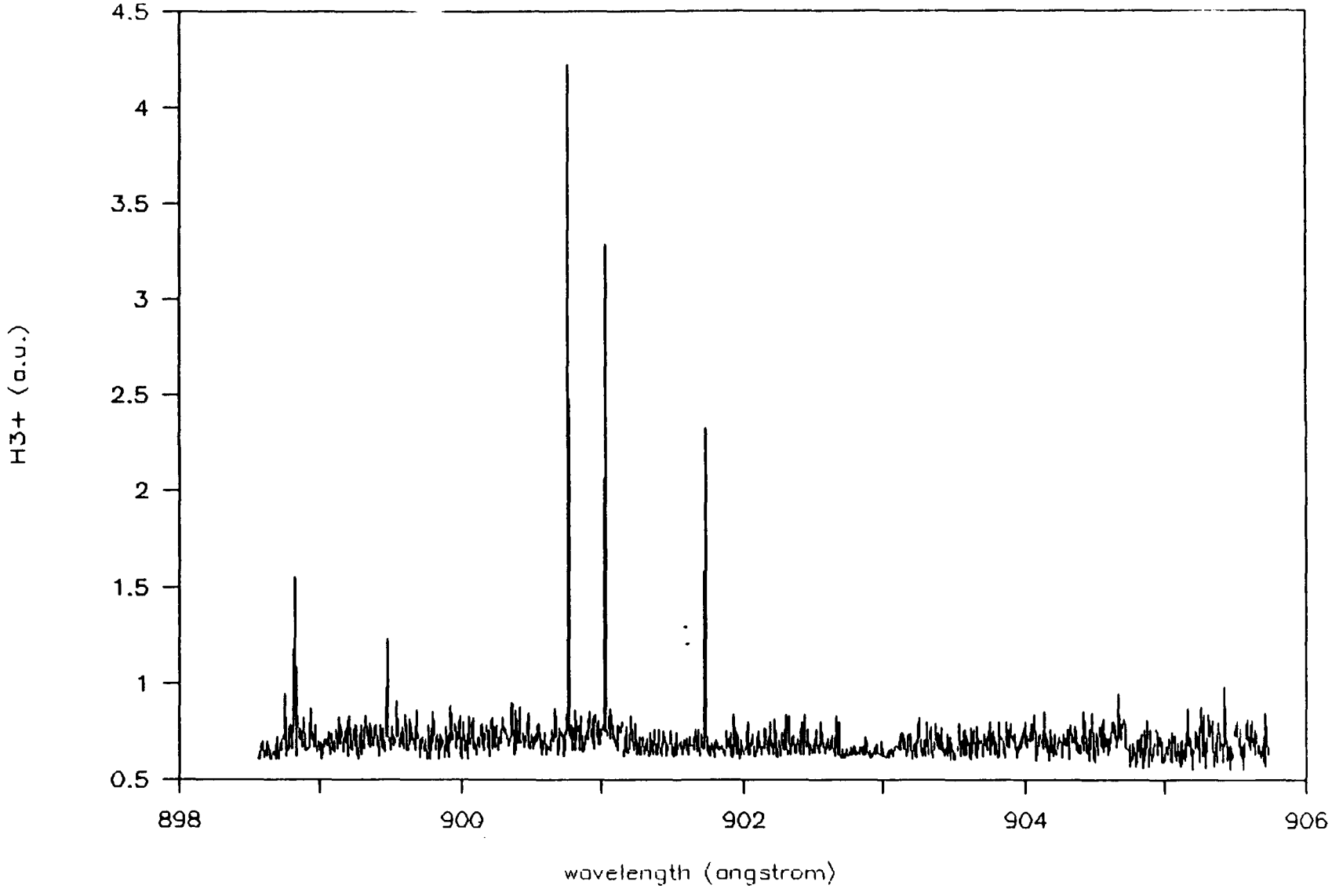

Figure 11. Photoionization spectrum of $(H_2)_2$ from 89.85 nm to 90.57 nm obtained by ion counting detection. Maximum intensity here is ten times stronger than that in figure 10, signalling stronger H_2 transitions in this region.

Table 3. Summary of observed photoionization peaks.

Position	Peak observed		
nm	LN_2 cooled nozzle mass 3	mass 2	room temp. mass 3
88.95	yes	yes	
88.99	yes	yes	
89.09	yes	yes	
89.32	yes	yes	
89.40	yes	yes	
89.42	yes	yes	
89.85	yes	-	yes
89.88	yes	yes	
89.95	yes	yes	
89.99	-	yes	
90.08	yes	yes	
90.11	yes	yes	
90.17	yes	yes	yes
90.47	-	yes	
90.53	-	yes	

IV. Infrared Spectroscopy of H_5^+

Studies in our laboratory of the vibrational predissociation spectra of mass selected ionic clusters of hydrogen, $H_3^+(H_2)_n$ (for n=1-6), prior to 1989 have yielded only vibrational information about these systems.[6] Vibrational transitions were observed and assigned to modes of the clusters associated with both the H_3^+ ion core of these systems and the H_2 solvent molecules. This vibrational structure demonstrated convergence at high n to a value close to that known for the vibrational frequency of H_2 in a solid hydrogen matrix. Although no rotational structure in this early work was observed, the data were most consistent with **ab-initio** results for the structures consisting of an H_3^+ core solvated by H_2 molecules.

The fact that no rotational structure was observed was particularly surprising as theoretical predictions for the rotational constants of the smallest cluster, H_5^+ , have values of A = 27 cm^{-1}, B = 3.21 and C = 3.18 cm^{-1} for the C_{2v} global minimum structure,[7] at the rather high level of theory 6s3p/CISD, considerably larger than the resolution of the laser system used. Possible explanations suggested for the unexpected result were homogeneous broadening of the transitions due to a particularly fast vibrational predissociation lifetime, or, spectral congestion due to high levels of internal excitation in the clusters being probed. This latter possibility was investigated by changing the means of generating the clusters from an

electron impact ionization source to a high pressure corona discharge source, known to produce vibrationally and rotationally colder clusters; rotational structure was not apparent for this source either.

In our studies, ions are produced in a high pressure (150-300 torr) discharge region and then undergo a supersonic expansion through a 70 μm nozzle for the formation of ionic clusters (see figure 12). It is necessary to keep the extraction field between nozzle and skimmer low (< 6 Volts/cm) in order to limit cluster dissociation and vibrational excitation in this region. The ionic cluster of interest is selected by means of a mass spectrometer and is held in a radio frequency ion trap while it interacts with a pulsed infrared laser (QuantaRay IR WEX). If the cluster ion absorbs sufficient energy from the laser, vibrational predissociation can take place, resulting in the loss of one or more solvent molecules. Spectra are obtained by using a second mass spectrometer to monitor the number of daughter ions produced as a function of laser wavelength.

Since the publication of the results of Okumura et al.[6], we have further reduced the internal excitation of H_5^+ by means of an expansion of helium and hydrogen in a 3:1 ratio rather than pure H_2, as used previously. From the observed spectrum, we estimate the rotational temperature of the hydrogen cluster ions to be about 20 K. The copper body of the corona discharge source itself was cooled to - 40° C. to

Schematics of the Ion Spectroscopy Machine

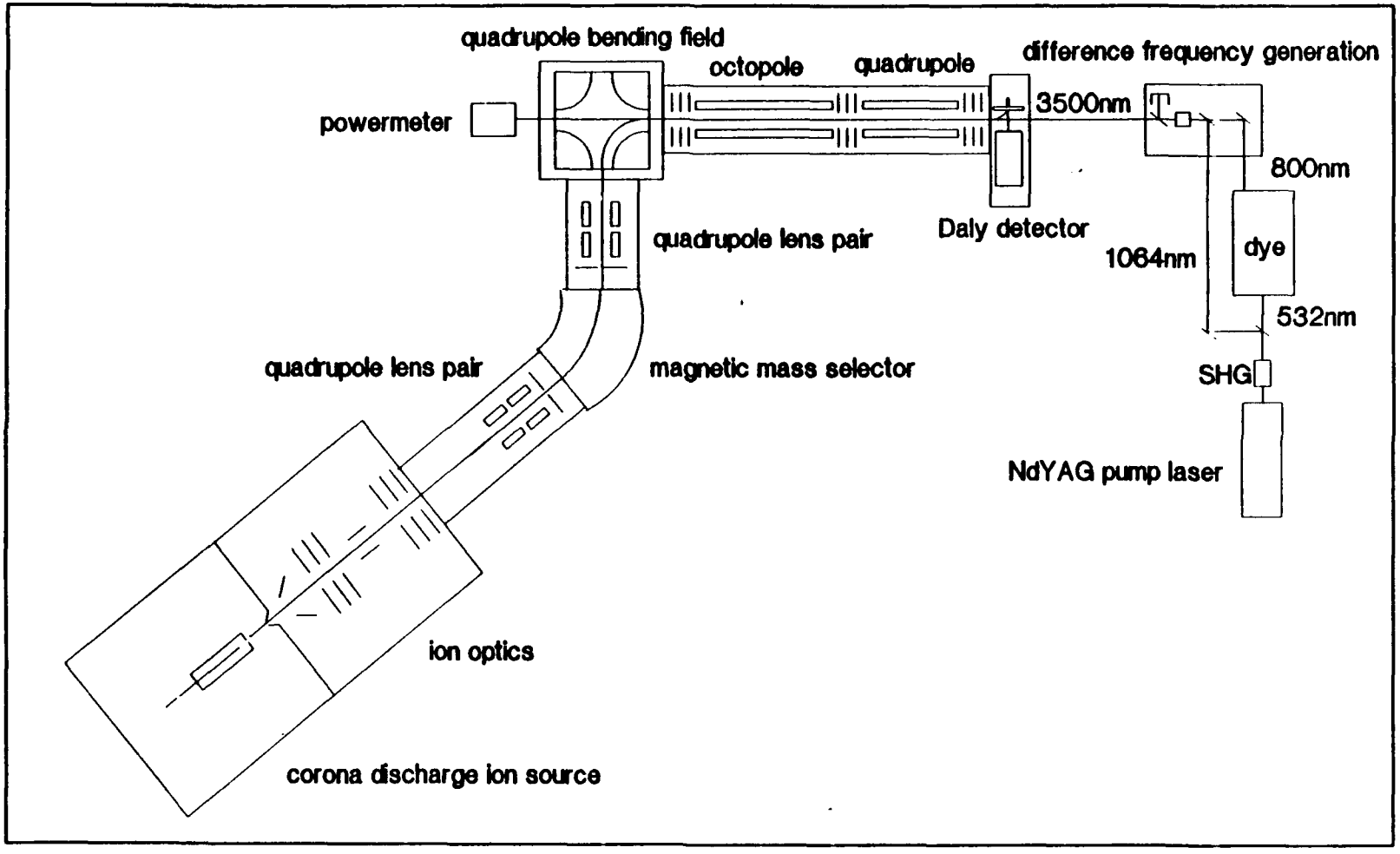

Figure 12. Schematic diagram of the cluster ion IR spectroscopy apparatus.

reduce the amount of vibrational excitation prior to expansion

This work represents the first direct observation of rotational structure in the hydrogen cluster ion systems. In spite of the superior rotational cooling, one still expects a substantial amount of spectral congestion due to hot bands, tunneling splittings and a homogeneous linewidth determined by the rate of the predissociation process.

Figure 13 shows a spectrum of the H_5^+ ν_2 band, obtained by averaging several scans with a laser limited resolution of 0.4 cm^{-1} and slightly smoothing the result to enhance the gross features. The maximum variation in the "fine structure" superimposed upon the band contour is only some 10% of the peak cross-section. Due to the inherently low product yield in this experiment, a low signal to noise ratio was inevitable even after days of signal averaging. The contour of the H_5^+ ν_1 band, which is centered at 3930 cm^{-1}, compares well with that of the ν_2 band (particularly on the high frequency side, where hot bands are less significant). This suggests that most of the "fine structure" features apparent in figure 13 are real.

There are obviously more features seen in figure 13 than are expected for jet-cooled rigid C_{2v} H_5^+ molecular ions. The width of some of these features seems to be quite narrow, probably laser-limited at 0.4 cm^{-1} laser linewidth. If so, it is certainly possible that the multitude of features is

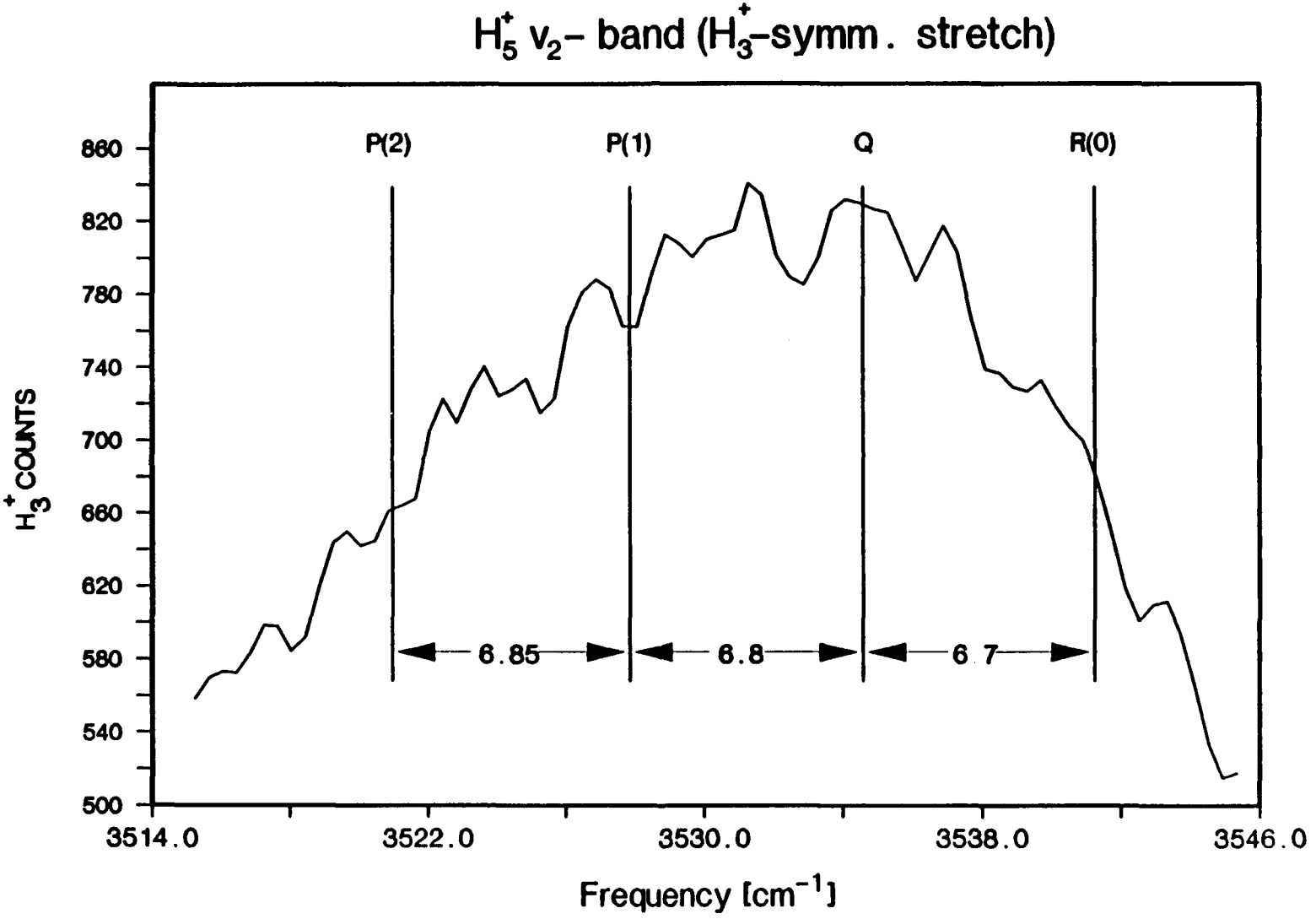

Figure 13. Vibrational predissociation, power normalized spectrum of the ν_2 band of H_5^+, taken with an infrared laser linewidth of 0.4 cm^{-1}. The assignments given are speculative and indicate the need for further investigation.

associated with tunneling splittings resulting from internal motions.

There are two internal motions in H_5^+ which are expected to be associated with a low potential barrier, roughly 0.3 kcal/mole.[2] These are (1) internal rotation of the H_2 subunit about the A axis of the complex and (2) tunneling of the central proton through a D_{2d} transition state such that the "H_2 molecule" subunit becomes part of the "H_3^+" subunit. A third internal motion is that of internal rotation of the "H_3^+" about its 3-fold axis, with a predicted barrier of about 4 kcal/mole. The tunneling splitting associated with this last motion should be relatively small. For a given barrier height, we expect motion (2) to produce larger splittings than motion (1), because of the larger effective mass involved in the tunneling process in the latter case. In figure 13, each rotational transition appears to be split by 2-3 cm^{-1}. In view of the above considerations and the suggestion by Yamaguchi **et al.**[7] that the barrier for motion (1) may be slightly higher than for (2), it seems most natural to attribute the splitting primarily to the tunneling motion of the central proton.

The tentative assignments given in figure 13 concern only P,Q or R branch and the total angular momentum quantum number, J, in the ground vibrational state. The center of a given transition, for example R(0), is at a local minimum of the intensity due to the 2-3 cm^{-1} splitting we have already mentioned.

We have investigated the D_5^+ spectrum also, since its spectrum can be expected to be simpler in appearance. This is so because of the usual order of magnitude decrease in tunneling splittings for deuterated species, and because the ratio of vibrational energy to dissociation energy is not so large in D_5^+ as compared to H_5^+. We have recorded the spectrum of the ν_1 band of D_5^+, shown in figure 14, for the first time. The "fine structure" is simpler this time, and the centers of rotational transitions P(1) and R(0), at least, can be taken to coincide with local intensity maxima. The spectrum is still quite congested, however, and it is tempting to argue that the predissociation process is partly responsible for its appearance. From the separation of the "prominent" peaks marked P(1) and R(0) (a highly tentative assignment), one deduces a value for (B+C)/2 of 1.73 ± 0.1 cm^{-1}. This is in agreement with the same parameter suggested for H_5^+ by the spectrum seen in figure 13, of 3.4± 0.2 cm^{-1} (because of the D/H mass ratio, the rotational constants of D_5^+ are, of course, half those of H_5^+). These values are in reasonable agreement with those obtained from the **ab-initio** structure calculations.[7] It is clear, however, that a great deal of arbitrariness is present in the "assignment" given. Because of this, it is necessary to improve the spectra.

Since the spectra of figures 13 and 14 were taken in the spring of 1989, we have attempted by several means to improve their quality. We tried an optical parametric amplification scheme to increase the infrared laser power,

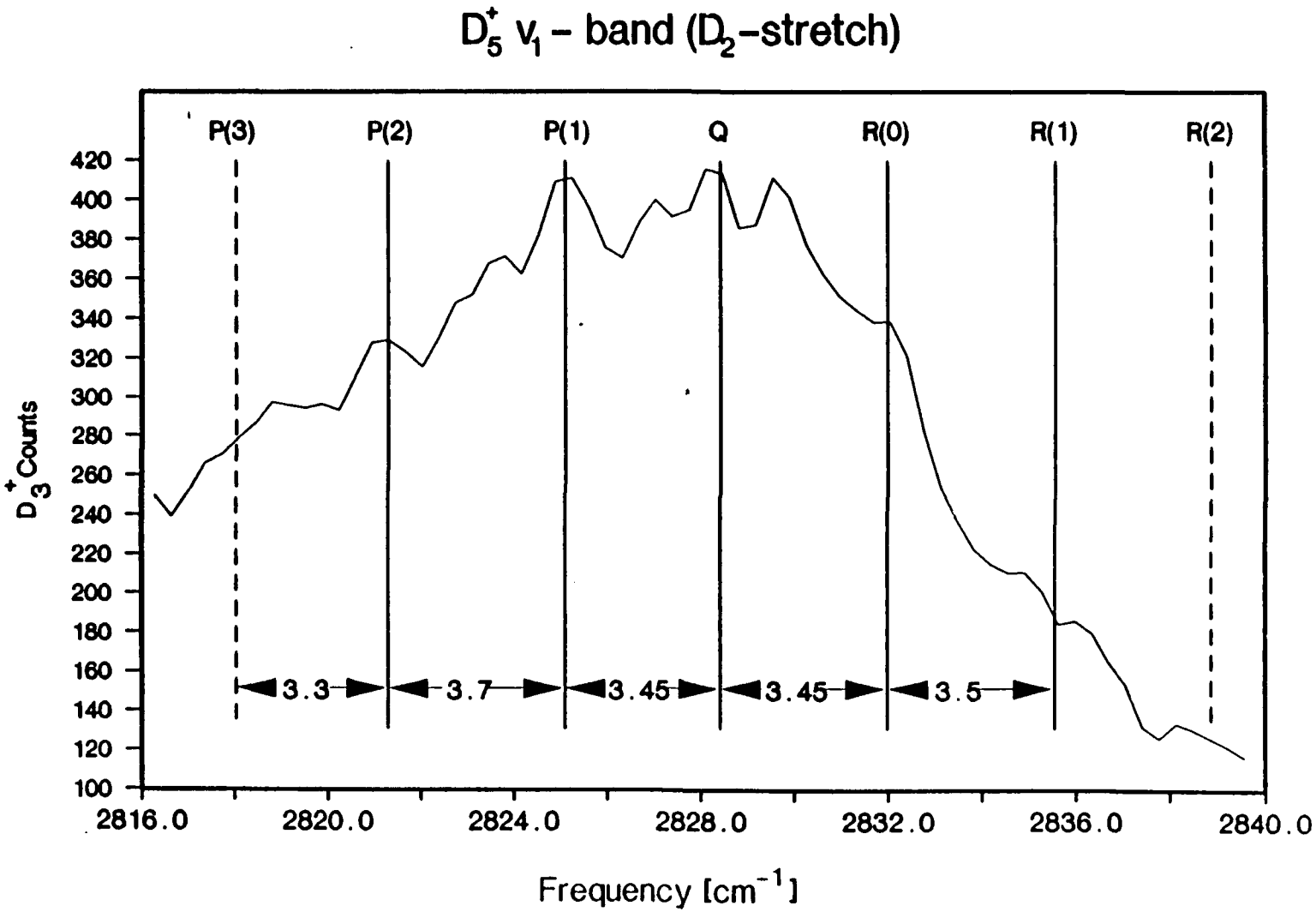

Figure 14. Vibrational predissociation, power normalized spectrum of the ν_1 band of D_5^+, taken with an infrared laser linewidth of 0.4 cm^{-1}. The signal to noise ratio is quite low, since the number of ion counts obtained at the absorption peak was only about 400. The assignments given are merely suggestive (see text).

but with limited success as the stability was degraded. A new injection seeded Quantel YG682-20 Nd:YAG laser and Lambda Physik FL3002E dye laser were purchased, in part with funds provided by the Air Force. These arrived in late January 1990. Since the computer control system and electronics of the experiment were upgraded at the same time, and familiarization with and integration of the new laser system into the existing experiment was required, the final phase of experimental testing was not achieved until May. A beautiful spectrum of $H_9O_4^+$ was obtained in the 3729-3732 cm^{-1} region under an etalon scan of the dye laser, quickly and with an impressive signal to noise ratio. The resolution of the dye laser was within the 0.04 cm^{-1} specification, and the data acquisition time for a given signal to noise ratio was reduced by a factor of about 7 as anticipated, when compared to the previous experiments.

The spectrum of D_5^+ was very recently recorded with the new laser system. The spectrum is reasonably similar to that obtained previously, but plagued by power and directional instabilities of the infrared for the high resolution (<0.2 cm^{-1}) scans. These effects, which produced somewhat regular fluctuations in power of about 20 %, were often similar in appearance to etalon effects. Because the instabilities involved beam quality and directional changes as well as power fluctuations, the signal could not be scaled by the power. While this problem now appears to be solved, the only reliable data available at the moment is

low resolution data. It is clear from the high resolution data, nevertheless, that the density of spectral transitions in the spectrum must be quite high, since the signal did not vary by more than 25 % within any 1 cm^{-1} interval.

A comparison of power normalized low resolution data taken with the two laser systems is given in figure 15. The dark trace was obtained with the new laser system. The peak signal was about 1700 D_3^+ counts, or four times that obtained previously with twice the integration time. Both traces have been slightly smoothed by identical means. While the two traces show a similar contour and some correspondence concerning individual transitions, there are significant differences between them. Of greatest importance, is the reduced prominence of the features labeled P(1) and Q in figure 14 and the appearance in the more recent data of new peaks, especially the one at about 2830.5 cm^{-1}. While it is possible that the spectrum appears differently due to different conditions, it seems more plausible that the signal to noise ratio is responsible for the variability. It is important to be cautious concerning spectral interpretation. The tenuous assignments of figures 13 and 14 should not be taken literally, as there is no clear evidence to warrant them. The numbers quoted for rotational constants are not established either. It is interesting to note, that in any of the spectra, one can imagine one or several series of peaks with approximately the correct rotational spacing. It does seem quite likely that there is

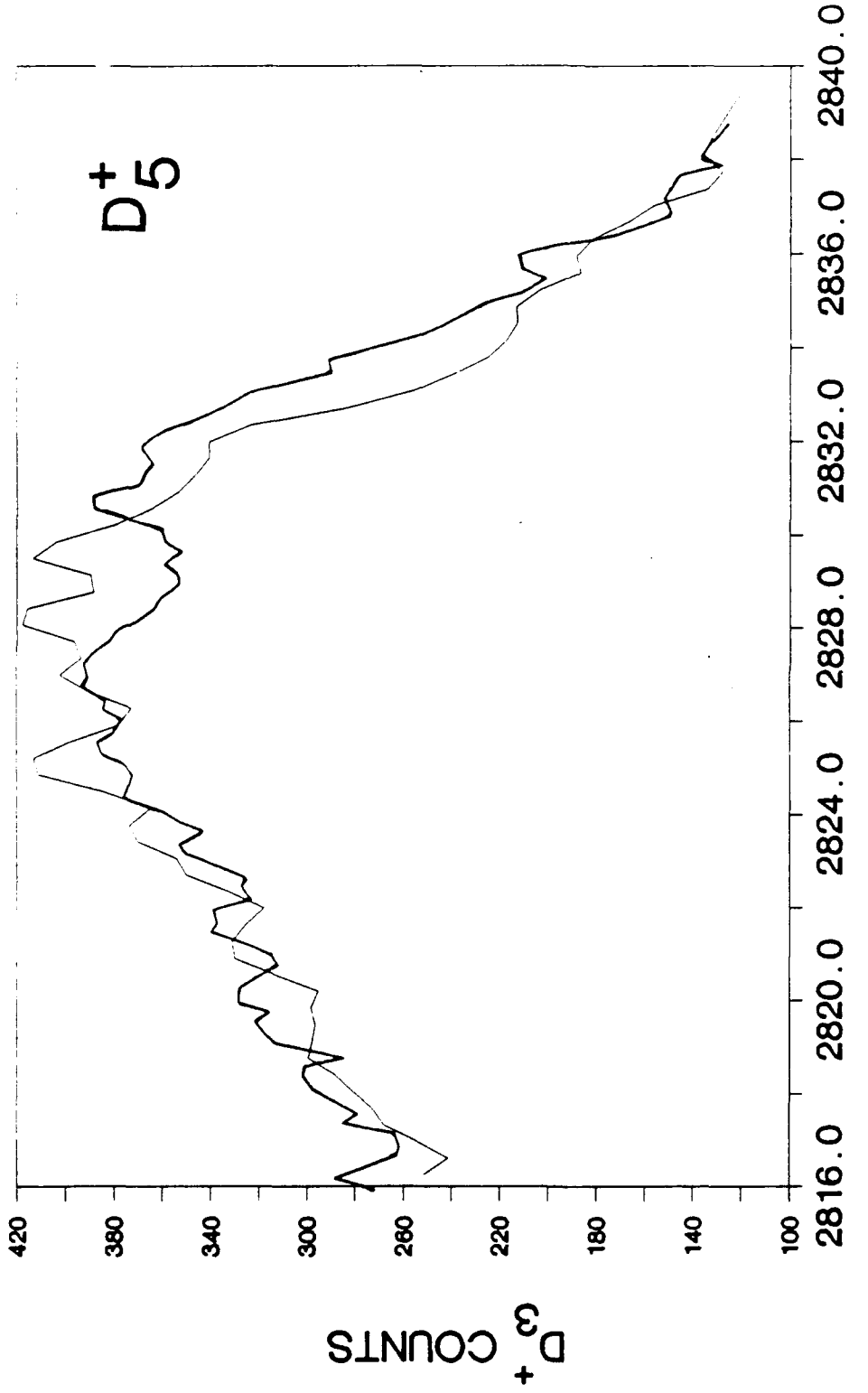

Figure 15. Comparison of D_5^+ data of figure 14 (light curve) with data obtained with the new laser system operated at ≈ 0.5 cm^{-1} resolution (dark curve). Accumulated ion counts at the peak was ≈ 1700 in the latter case, resulting in an expected signal to noise ratio improvement by a factor of 2 (see text for discussion).

an extensive mixing with background states, leading to a high density of spectral transitions. At the same time, the similarity between H_5^+ ν_1 and ν_2 bands and the D_5^+ ν_1 band, together with the narrow widths of the bands, shows that the interaction matrix elements coupling background states cannot typically be more than a few wavenumbers. A comparison of H_5^+ and D_5^+ spectra also suggests that hot band contributions are important, with the D_5^+ spectrum showing a greater contribution.

For H_7^+ and the larger clusters, bandwidths increase,[6] possibly indicating that predissociative effects have a greater influence on the spectrum. Even the H_2 stretch in $H_3N_2^+$ we have recently observed, seems to be broadened by a few wavenumbers. The same is true to a greater extent for overtone bands of H_5^+.[8] It is quite plausible that predissociative effects are not necessary to explain these phenomena. The broadening may be dependent on the density of states and other factors as is the case for high overtone spectra of C-H oscillators, with predissociation playing only a minor role.

The obvious H_5^+ band to study for more rigorous information is the relatively intense H_3^+ antisymmetric stretch, which lies in the 6 μm region - below the dissociation threshold. The spectroscopy of that band is likely to reveal sharp, resolvable features which will be much easier to understand and obtain concrete information from. In addition, it is quite conceivable that we can

eventually study the H_3^+ antisymmetric stretch in H_5^+. This stretching state lies below the dissociation threshold. We are directing our efforts towards this goal and have nearly finished the design phase for construction of a multiple pass Raman cell which should provide more than enough pulse energy to accomplish this task. Such a project would have been nearly unthinkable without the new laser system.

An attempt to record the spectrum of $H_2D_3^+$ failed, due to poor signal to noise ratio. There are, of course, several isomers of the ion, and predissociation of any one isomer probably occurs into all three of the possible channels. Considering that the presence of both H and D in the discharge results in the formation of a distribution of ions containing all possible permutations involving H and D, the combined loss of signal from all effects is about one order of magnitude.

Future plans do include a more careful recording of the ν_1 and ν_2 bands of H_5^+ at 0.04 cm^{-1} resolution, with careful frequency calibration.

V. References:

1. C.A. Nicolaides, G. Theodorakopoulos, and I.D. Petsalakis, **J. Chem. Phys. 80**, 1075 (1984) and C.A. Nicolaides, I.D. Petsalakis, and G. Theodorakopoulos, **J. Chem. Phys. 81**, 748 (1984).

2. High energy density materials contractors conference, AFOSR, Feb 28-Mar 2, 1988, Newport Beach, CA

3. S.L. Anderson, T. Hiroka, P.W. Tiedemann, B.H. Mahan, and Y.T. Lee, **J. Chem. Phys. 73**, 4779 (1980).

4. E. Cromwell, T. Trickl, Y.T. Lee, and A.H. Kung, **Rev. Sci. Inst. 60(9)**, 2888 (1989)

5. A. H. Kung, T. Trickl, N.A. Gershenfeld, and Y.T. Lee, **Chem. Phys. Lett. 144**, 427 (1988).

6. M. Okumura, L.I. Yeh and Y.T. Lee, **J. Chem. Phys. 88**, 79 (1988); **83**, 3705 (1985).

7. Y. Yamaguchi, J.F. Gaw, R.B. Remington and H.F. Schaefer III, **J. Chem. Phys. 86**, 5072 (1987).

8. Young Bae, submitted to Chem. Phys. Lett.

VI. Abstracts of reprints and preprints.

See attached.

State-Selective Detection of H_2 by 1 + 1 REMPI via the $C^1\Pi_u(v' = 0, J')$ States

A.H. Kung, T. Trickl, N.A. Gershenfeld and Y.T. Lee
Department of Chemistry, University of California
Berkeley, California 94720

It is shown that there are some advantages to determining ground state population distribution of H_2 by 1 + 1 REMPI using the $C^1\Pi_u(v' = 0)$ state as the intermediate state. The state distribution can be deduced more directly from the ion signal; in addition, a much improved sensitivity of $< 1.7 \times 10^5$ molecules/cm^3 per quantum state is achieved.

Chem. Phys. Lett. **144**, 427 (1988).

Dynamics of Electronic Energy Quenching: The Reaction of $H_2(B)$ + He

Charles D. Pibel, Karen L. Carleton and C. Bradley Moore

Department of Chemistry, University of California

Berkeley, California 94720

The room temperature rate constants for quenching of the fluorescence of H_2, HD, and D_2 B $^1\Sigma_u^+$ by ^{4}He have been measured as a function of the initially excited rotational and vibrational level of the hydrogen molecule. The effective quenching cross sections increase with increasing vibrational energy from about 1 $Å^2$ up to a maximum of about 6 $Å^2$. The effective cross sections for D_2 (B, v'=0) were independent of the rotational level excited for $0 < J' \leq 7$,and the cross sections for (v'=0,J'=0) were about 80% of the values for (v'=0,J'>0) for all three isotopes studied. Quenching occurs via formation of an electronically excited $(H_2He)^*$ collision complex followed by crossing to the repulsive $H_2(X)$-He potential energy surface. The vibrational state dependence of the quenching cross sections fits a vibrationally adiabatic model for complex formation. From the vibrational state dependence of the quenching cross section, the barrier height for the quenching reaction is found to be 250 ± 40 cm^{-1}, and the difference in the H-H stretching frequencies between $H_2(B)$ and the H_2-He complex at the barrier to reaction is 140 ± 80 cm^{-1}. Both values are substantially smaller than results from ab initio calculations. The rotational state dependence of the quenching cross sections suggests that quenching occurs with H_2 rotating in a plane perpendicular to the relative velocity vector, in qualitative agreement with the rotational anisotropy of the $H_2(B)$-He ab initio electronic potential energy surface.

J. Chem. Phys. **93**, 323 (1990).

Molecular Angular Momentum Reorientation of Electronically Excited Hydrogen ($B^1\Sigma_u^+$)

Charles D. Pibel and C. Bradley Moore
Department of Chemistry, University of California
Berkeley, California 94720

The room temperature rate constants for molecular angular momentum reorientation of H_2, HD and D_2 ($B\ ^1\Sigma_u^+$, $v'=0$, $J'=1$, $M_J'=0$) in collisions with He, Ne, Ar and $H_2(X\ ^1\Sigma_g^+)$ have been measured. The effective cross sections for changing M_J' in collisions of H_2, HD, D_2 with He and Ne were found to be about 30 $Å^2$ and were nearly the same for each isotope and with He and Ne as collision partners. The measured He-H_2(B) reorientation cross section is about 50 % larger than the cross section calculated with a simple semiclassical model using a potential that approximates the ab initio data for the H_2(B)-He potential energy surface. The cross sections for reorientation of HD and D_2 in collisions with Ar were found to be 10.6 ± 2.0 and 13.9 ± 3.0 $Å^2$, respectively. The smaller cross section is due to the dominant role played by quenching of the electronic energy of molecular hydrogen in collisions with Ar. The reorientation of D_2(B) in collisions with room temperature H_2(X) occurs with a 7.6 ± 3.4 $Å^2$ cross section. The small cross section for reorientation of the angular momentum is again due to the dominance of quenching in the collision dynamics.

J. Chem. Phys. (in press) (1990).